JGP Journal of General Physiology

ARTICLE

Function of mammalian M-cones depends on the level of CRALBP in Müller cells

Alexander V. Kolesnikov[1], Philip D. Kiser[2,3,4], Krzysztof Palczewski[2,3,5], and Vladimir J. Kefalov[1]

Cone photoreceptors mediate daytime vision in vertebrates. The rapid and efficient regeneration of their visual pigments following photoactivation is critical for the cones to remain photoresponsive in bright and rapidly changing light conditions. Cone pigment regeneration depends on the recycling of visual chromophore, which takes place via the canonical visual cycle in the retinal pigment epithelium (RPE) and the Müller cell–driven intraretinal visual cycle. The molecular mechanisms that enable the neural retina to regenerate visual chromophore for cones have not been fully elucidated. However, one known component of the two visual cycles is the cellular retinaldehyde-binding protein (CRALBP), which is expressed both in the RPE and in Müller cells. To understand the significance of CRALBP in cone pigment regeneration, we examined the function of cones in mice heterozygous for *Rlbp1*, the gene encoding CRALBP. We found that CRALBP expression was reduced by ∼50% in both the RPE and retina of *Rlbp1*$^{+/-}$ mice. Electroretinography (ERG) showed that the dark adaptation of rods and cones is unaltered in *Rlbp1*$^{+/-}$ mice, indicating a normal RPE visual cycle. However, pharmacologic blockade of the RPE visual cycle revealed suppressed cone dark adaptation in *Rlbp1*$^{+/-}$ mice in comparison with controls. We conclude that the expression level of CRALPB specifically in the Müller cells modulates the efficiency of the retina visual cycle. Finally, blocking the RPE visual cycle also suppressed further cone dark adaptation in *Rlbp1*$^{-/-}$ mice, revealing a shunt in the classical RPE visual cycle that bypasses CRALBP and allows partial but unexpectedly rapid cone dark adaptation.

Introduction

The regeneration of photobleached visual pigments in retinal photoreceptors, rods and cones, underlies sustained vision in all vertebrate species. In these primary visual neurons, the initial absorption of a photon by the rod pigment (rhodopsin) or different cone pigments triggers the photoconversion of the visual chromophore, 11-cis-retinal, to its all-trans form. This isomerization activates the phototransduction cascade and generates the physiological light response. All-trans-retinal is then released from photoreceptors and recycled back to 11-cis-retinal via either the canonical retinal pigment epithelium (RPE)-driven visual cycle (which delivers chromophore to both rods and cones) or the Müller cell–mediated retina visual cycle serving the cones exclusively (reviewed by Wang and Kefalov, 2011; Tang et al., 2013; Kiser et al., 2014). Direct photoisomerization of phospholipid-bound all-trans-retinal to 11-cis-retinal with blue light, similar to that occurring within invertebrate opsins, has also been reported (Kolesnikov et al., 2006; Kaylor et al., 2017).

The cone-specific pathway and its critical molecular players are active areas of research (Kaylor et al., 2013; Kaylor et al., 2014; Sato and Kefalov, 2016; Sato et al., 2017; Xue et al., 2017; Kiser et al., 2019). A common feature of the classic RPE and intraretinal visual cycles is their complement of chromophore-binding proteins facilitating the process of recycling of very hydrophobic retinoids. One of these, cellular retinaldehyde-binding protein (CRALBP), is essential for mammalian cone pigment regeneration (Saari et al., 2001; Xue et al., 2015).

CRALBP is abundantly expressed, both in Müller cells of the retina and in the RPE (Bunt-Milam and Saari, 1983; Saari et al., 2001), and its complete elimination severely compromises the cone-mediated daylight vision and dark adaptation of M-cones in mice (Xue et al., 2015). Structurally, CRALBP is a 36-kD globular protein capable of adopting two distinct conformational states for the binding and intracellular transport of both 11-cis-retinol and 11-cis-retinal (Futterman et al., 1977; Saari and Bredberg, 1987; Liu et al., 2005; He et al., 2009).

Numerous mutations in human CRALBP (encoded by the *RLBP1* gene) have been implicated in several retinal diseases, including autosomal recessive retinitis pigmentosa (Maw et al.,

[1]Department of Ophthalmology and Visual Sciences, Washington University School of Medicine, St. Louis, MO; [2]Department of Physiology and Biophysics, School of Medicine, University of California, Irvine, Irvine, CA; [3]Department of Ophthalmology, Gavin Herbert Eye Institute, Center for Translation Vision Research, School of Medicine, University of California, Irvine, Irvine, CA; [4]Research Service, VA Long Beach Healthcare System, Long Beach, CA; [5]Department of Chemistry, School of Medicine, University of California, Irvine, Irvine, CA.

Correspondence to Vladimir J. Kefalov: kefalov@wustl.edu.

1997), retinitis punctata albescens (Morimura et al., 1999), Bothnia dystrophy (Burstedt et al., 1999; Burstedt et al., 2001; Burstedt et al., 2003), fundus albipunctatus (Katsanis et al., 2001; Naz et al., 2011), and Newfoundland rod-cone dystrophy (Eichers et al., 2002). These visual disorders are characterized by early loss of scotopic vision and may be followed by functional defects in the macula (Thompson and Gal, 2003). Many of their characteristic features, such as impaired visual cycle, attenuated levels of bisretinoid lipofuscin fluorophores, progressive RPE atrophy, and photoreceptor degeneration, are replicated in a mouse model of CRALBP deficiency (Lima de Carvalho et al., 2020).

In the RPE, it is believed that CRALBP binds 11-cis-retinol produced by retinoid isomerase RPE65 (Winston and Rando, 1998; Stecher et al., 1999) and facilitates its subsequent oxidation to 11-cis-retinal, which is catalyzed by RDH5 and other cis-specific retinol dehydrogenases (Saari and Bredberg, 1982; Saari et al., 1994). Whereas a specific function of CRALBP in Müller cells is still unclear, there it could perform a similar role of the acceptor for 11-cis-retinol generated by a yet unidentified isomerase (Kiser et al., 2019) or by a photic mechanism driven by retinal G protein–coupled receptor opsin coupled to retinol dehydrogenase 10 (Morshedian et al., 2019), as has recently been suggested for the RPE (Zhang et al., 2019).

Several important issues relevant to the role of CRALBP in cone photoreceptor physiology remain to be addressed. First, the importance of Müller cell CRALBP expression level in modulating the supply of visual chromophore to cones and in their operation in bright light and dark adaptation in vivo has yet to be determined. Second, the ability of mouse M-cones to moderately restore their sensitivity after exposure to intense light even in the complete absence of CRALBP (Xue et al., 2015) raises the possibility of a potential CRALBP-independent mechanism of cone pigment regeneration. Third, compromised delivery of chromophore from the RPE visual cycle can also delay the dark adaptation of cones, possibly due to the interplay between the two visual cycle pathways (Kolesnikov et al., 2015; Kiser et al., 2018). Resolving these issues requires a more thorough examination of M-cone function while modulating both CRALBP expression and the contribution of newly regenerated chromophore from the RPE and retinal visual cycles. In addition, it is important to assess whether the amount of CRALBP in the RPE modulates the supply of 11-cis-retinal to rods as well. Here, we investigated these questions by using mice with reduced (halved) or ablated CRALBP expression and/or pharmacologically blocked regeneration of visual chromophore.

Materials and methods

Animals

CRALBP-deficient (*Rlbp1*$^{-/-}$) mice were described previously (Saari et al., 2001). Rod transducin α-subunit–knockout (*Gnat1*$^{-/-}$) mice lacking rod signaling (Calvert et al., 2000) were used as controls in all cone physiological experiments. The two lines were also crossed to generate *Rlbp1*$^{-/-}$*Gnat1*$^{-/-}$ and *Rlbp1*$^{+/-}$*Gnat1*$^{-/-}$ animals (for cone recordings) or *Rlbp1*$^{+/-}$*Gnat1*$^{+/-}$ and control *Rlbp1*$^{+/+}$*Gnat1*$^{+/-}$ lines (for rod recordings). All mice used in this study were homozygous for the Leu450 allele of *Rpe65* as determined by a genotyping protocol published elsewhere (Grimm et al., 2004) and free of *Crb1/rd8* mutation (Mattapallil et al., 2012). Young adult animals of either sex (2–4 mo old) were tested in all experiments. Mice were provided with standard chow (LabDiet 5053; LabDiet, Purina Mills) and maintained under a 12-h light (10–20 lux)/12-h dark cycle. All experiments were approved by the Washington University Animal Studies Committee.

Western blotting

Whole mouse eyes or isolated retinas were retrieved from storage at −80°C and placed in PBS containing a 1× concentration of protease inhibitors (Bimake). Individual eyes were subjected to 30 passes in a Dounce homogenizer, and isolated retinas were lysed by sonication. Protein concentrations of the resulting lysates were determined using the Bradford assay (Pierce) by reading the sample 595-nm absorbances along with those of BSA standards together in a FlexStation 3 plate reader (Molecular Devices). The protein concentrations were equalized across each of the samples by the addition of lysis buffer. The lysates were then stored at −80°C until needed for further analysis. Protein samples of 35 µg (whole eyes) or 7 µg (isolated retinas) in standard loading buffer were separated by SDS-PAGE on a 12% gel in Tris-glycine running buffer. The proteins were then transferred onto a 0.45-µm polyvinylidene difluoride membrane using an eBlot semidry transfer system (GenScript) according to the manufacturer's instructions. The membrane was dried for 1 h and then rewetted with 100% methanol followed by the addition of a blocking mixture consisting of 5% nonfat milk in PBS containing 0.05% Tween 20 (PBST; Sigma-Aldrich). After 1-h incubation at room temperature (RT) with gentle rocking, the membrane was transferred into 2 ml of 5% nonfat milk in PBST. Rabbit anti-CRALBP (UW55) and mouse anti-tubulin (Ab7291; Abcam) antibodies were then added to the membrane incubation mixture at dilutions of 1:2,000 and 1:5,000, respectively. After a 1-h incubation at RT with gentle rocking, the primary antibody mixture was decanted, and the membrane was washed three times with 5 ml PBST, each time for 5 min. The membrane was then incubated in 5% nonfat milk PBST mixture containing goat anti-rabbit (IRDye 800CW; LI-COR Biosciences) and donkey anti-mouse (IRDye 680RD; LI-COR Biosciences) secondary antibodies, both at 1:20,000 dilution. After a 1-h incubation at RT with gentle rocking, the secondary antibody mixture was decanted, and the membrane was washed three times with 5 ml PBST, each time for 5 min. The membrane was then incubated in PBS for 3 min and then analyzed for fluorescent labeling using the 700-nm and 800-nm channels on a LI-COR Odyssey blot imager (LI-COR Biosciences). The image contrast and coloring were globally adjusted using Adobe Photoshop. CRALBP signals were normalized to those of the tubulin loading controls using ImageJ software (Schneider et al., 2012).

Transretinal (ex vivo electroretinography [ERG]) recordings from isolated retinas

Mice were dark adapted overnight and then euthanized by asphyxiation with a rising concentration of CO_2, and a whole retina was removed from each mouse eyecup under infrared illumination and stored in oxygenated aqueous L15 (13.6 mg/ml, pH 7.4; Sigma-Aldrich) solution containing 0.1% BSA at RT. The

retina was mounted on filter paper with the photoreceptor side up and placed in a perfusion chamber between two electrodes connected to a differential amplifier. The tissue was perfused with Locke's solution containing 112.5 mM NaCl, 3.6 mM KCl, 2.4 mM $MgCl_2$, 1.2 mM $CaCl_2$, 10 mM HEPES, pH 7.4, 20 mM $NaHCO_3$, 3 mM Na succinate, 0.5 mM Na glutamate, 0.02 mM EDTA, and 10 mM glucose. This solution was supplemented with 1.5 mM L-glutamate and 40 µM DL-2-amino-4-phosphonobutyric acid to block post-synaptic components of the photoresponse (Sillman et al., 1969) and with 70 µM $BaCl_2$ to suppress the slow glial PIII component (Nymark et al., 2005). The perfusion solution was continuously bubbled with a 95% O_2/5% CO_2 mixture and heated to 36–37°C.

Light stimulation was applied in 20-ms test flashes of calibrated 505-nm LED light. The stimulating light intensity was controlled by a computer in 0.5–log-unit steps. Intensity–response relationships were fitted with Naka-Rushton hyperbolic functions as follows:

$$R = \frac{R_{\max} \cdot I^n}{I^n + I_{1/2}^n},$$

where R is the transient-peak amplitude of the response, R_{max} is the maximal response amplitude, I is the flash intensity, n is the Hill coefficient (exponent), and $I_{1/2}$ is the half-saturating light intensity. In experiments designed to monitor the post-bleach recovery of cone a-wave flash sensitivity (S_f; see definition below), >90% of M-cone visual pigment was bleached with a 3-s exposure to 505-nm light. The bleached fraction was estimated from the following equation:

$$F = 1 - \exp(-I \cdot P \cdot t),$$

where F is the fraction of pigment bleached, t is the duration of the light exposure (in seconds), I is the bleaching light intensity of 505-nm LED light (1.6×10^8 photons µm^{-2} s^{-1}), and P is the photosensitivity of mouse cones at the wavelength of peak absorbance (7.5×10^{-9} µm^2), adopted from Nikonov et al. (2006). Photoresponses were amplified by a differential amplifier (DP-311; Warner Instruments), low-pass filtered at 300 Hz (eight-pole Bessel), digitized at 1 kHz, and stored on a computer for further analysis. S_f was calculated from the linear part of the intensity–response curve as follows:

$$S_f = R/(R_{max} \cdot I),$$

where R is the cone a-wave dim flash response amplitude, R_{max} is the maximal response amplitude for that retina, and I is the flash strength. Data were analyzed with Clampfit 10.4 and Origin 8.5 software.

In vivo ERG

Dark-adapted mice were anesthetized with an intraperitoneal (IP) injection of a mixture of ketamine (100 mg/kg) and xylazine (20 mg/kg). Pupils were dilated with a drop of 1% atropine sulfate. Mouse body temperature was maintained at 37°C with a heating pad. ERG responses were measured from both eyes by contact corneal electrodes held in place by a drop of Gonak solution. Full-field ERG scans were recorded with the UTAS BigShot apparatus (LKC Technologies) using Ganzfeld-derived test flashes of calibrated green 530-nm LED light (within a range from 0.24 cd•s/m^2 to 23.5 cd•s/m^2, depending on the mouse line and experimental conditions). For cone recordings, the cone b-wave S_f, calculated similarly to the a-wave S_f in ex vivo ERG recordings, was first determined in the dark from the dim flash response amplitude normalized to the maximal b-wave amplitude, obtained with the brightest white light stimulus of the Xenon Flash tube (700 cd•s/m^2). Then, bright green background Ganzfeld illumination (300 cd/m^2; estimated to bleach ∼0.8% M-cone pigment s^{-1}) was applied continuously for 30 min, and the cone b-wave S_f change was monitored during this period of light exposure. Within the last 5 min of this illumination, mice were reanesthetized with a smaller dose of ketamine (approximately one-half of the initial dose), and a 1:1 mixture of PBS and Gonak solution was gently applied to the eyes with a plastic syringe to protect them from drying and to maintain electrode contacts. Finally, the remaining M-cone pigment was nearly completely bleached by a 35-s exposure to additional bright light delivered by a 520-nm LED focused at the surface of the mouse eye cornea that produced ∼1.3×10^8 photons µm^{-2} s^{-1}. The bleaching fraction was estimated by the formula $F = 1 - \exp(-I \cdot P \cdot t)$ defined above. After the bleach, the recovery of cone b-wave S_f was followed in darkness for up to 1 h (with one more reanesthesia in the middle of that period). In a subset of experiments, the 30-min Ganzfeld illumination step was omitted, and S_f recovery was determined after an acute >90% cone pigment bleach (520-nm LED; 35 s) was applied to dark-adapted animals.

Rod dark adaptation tests were performed in a similar way in mice derived on a *Gnat1*$^{+/-}$ genetic background. Rod a-wave S_f was first determined in the dark and normalized to the maximal a-wave amplitude (A_{max}) produced with the brightest green light stimulus (23.5 cd•s/m^2). The post-bleach recovery of the rod ERG A_{max} and S_f was then monitored after an acute >90% rhodopsin bleach (520-nm LED; 35 s; P = 5.7×10^{-9} µm^2 for mouse rods; Woodruff et al., 2004).

MB-001, prepared as per Kiser et al. (2015), was dissolved before each experiment in DMSO to 4 µg/µl, and 50 µl of this solution were administered by IP injection in the dark, followed by a period of 20–24 h of dark adaptation before ERG recordings. Control mice were injected with 50 µl DMSO and processed in the same way as drug-treated animals.

Statistics

For all experiments, data were presented as mean ± SEM. Western blotting and dark-adapted photoresponse data were analyzed using the independent two-tailed Student's t test. Post-bleach recovery time-course data were analyzed with the repeated-measures two-factor ANOVA test. The extra sum-of-squares F test was used to compare parameters derived from nonlinear regression analysis. In all cases, a P value < 0.05 was considered statistically significant. Statistical tests were performed using either Sigmaplot (Systat) or GraphPad software.

Results

Reduced expression of CRALBP does not affect M-cone photosensitivity in mice

To determine whether the level of CRALBP in mammalian eyes is critical for the normal function of M-cone photoreceptors, we

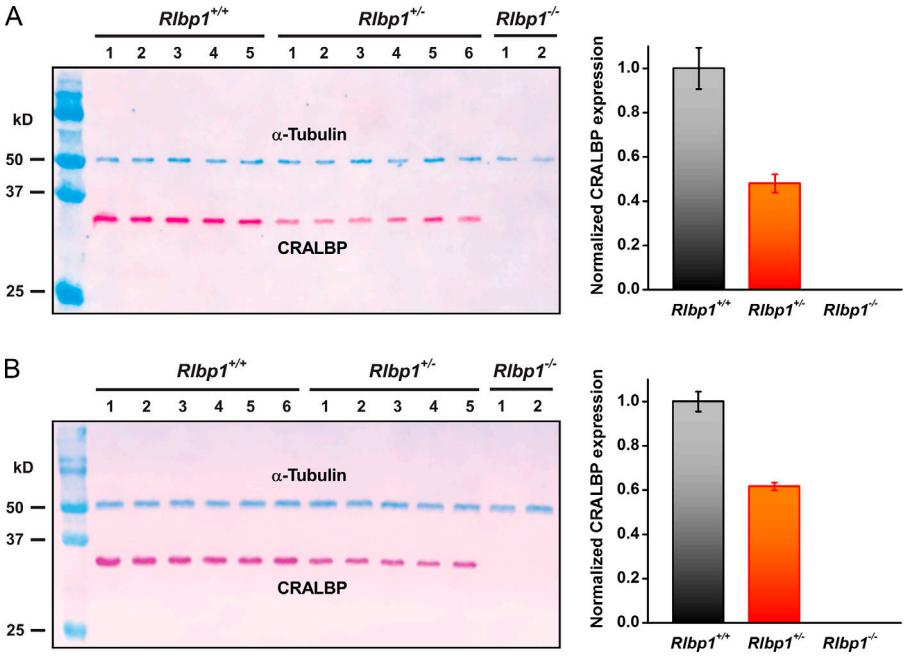

Figure 1. **Quantification of CRALBP expression in mouse eyes and isolated retinas. (A)** Left: Immunoblot of SDS-PAGE–separated proteins from whole-eye lysates of mice with the indicated genotypes. Right: Quantification of the α-tubulin–normalized, CRALBP-associated fluorescent signals reveals a 50% reduction ($P < 0.05$, Student's t test) in CRALBP expression in *Rlbp1*$^{+/-}$ ($n = 6$) animals compared with *Rlbp1*$^{+/+}$ ($n = 5$) controls. No CRALBP signal was detected in eyes from *Rlbp1*$^{-/-}$ ($n = 2$) animals. Error bars represent SEMs. **(B)** Left: Immunoblot of SDS-PAGE–separated proteins from isolated retinal lysates of mice with the indicated genotypes. Right: Quantification of the α-tubulin–normalized, CRALBP-associated fluorescent signals reveals an ∼40% reduction ($P < 0.05$, Student's t test) in CRALBP expression in *Rlbp1*$^{+/-}$ ($n = 5$, two retinas per sample) animals compared with *Rlbp1*$^{+/+}$ ($n = 6$, two retinas per sample) controls. No CRALBP signal was observed in retinas from *Rlbp1*$^{-/-}$ ($n = 2$) animals. Error bars represent SEMs.

sought to use a mouse model in which the total amount of this important visual cycle protein is reduced substantially. Therefore, we generated a mouse line heterozygous for the gene encoding CRALBP (*Rlbp1*$^{+/-}$). In addition, to facilitate cone recordings, these animals were derived on the *Gnat1*$^{-/-}$ genetic background. The lack of the transducin α-subunit eliminates the rod component of the light response in mice without affecting cone morphology or function (Calvert et al., 2000). Western blotting analysis demonstrated that the expression of CRALBP in whole *Rlbp1*$^{+/-}$ mouse eyes was reduced by 50% (Fig. 1 A). Because this protein is abundantly expressed in both the Müller cells of the retina and RPE (Bunt-Milam and Saari, 1983; Saari et al., 2001), we also quantified its level in isolated retina samples. Again, we found ∼40% decrease in expression of CRALBP in retinas from *Rlbp1*$^{+/-}$ animals (Fig. 1 B), suggesting similar reduction of its expression in RPE and Müller cells. As expected, no CRALBP protein was detected in the eyes or retinas from *Rlbp1*$^{-/-}$ mice (Fig. 1, A and B, right).

We then recorded a series of M-cone transretinal (ex vivo ERG) responses elicited by test flashes of increasing light intensity (Fig. 2, A and B). The recordings were performed following the overnight dark adaptation of tested animals from their isolated retinas in the presence of post-synaptic blockers. Our analysis was limited to M-cones, which can be selectively stimulated with visible green light. We found that the maximal cone response amplitude in retinas of 2-mo-old *Rlbp1*$^{+/-}$ mice was indistinguishable from that in age-matched *Gnat1*$^{-/-}$ controls (Fig. 2, A–C). The cone photosensitivity in *Rlbp1*$^{+/-}$ mice (defined as $I_{1/2}$) was also unaltered (Fig. 2 C).

Surprisingly, we found that M-cone dim flash responses in CRALBP-reduced mice were accelerated as compared with those in control animals (Fig. 2 D). While the activation phase of cone phototransduction estimated from the rising part of the responses was similar in the two strains, the inactivation phase of the cascade was noticeably faster in *Rlbp1*$^{+/-}$ mice. The time-to-peak values of cone dim flash responses were 87 ± 3 ms (control; $n = 11$) and 60 ± 2 ms (*Rlbp1*$^{+/-}$*Gnat1*$^{-/-}$; $n = 9$; $P < 0.05$); yet, both were within the range of 60–90 ms described for mouse cones previously (Nikonov et al., 2006). The average dim flash recovery time constants determined from single-exponential fits to the falling phase of cone photoresponses after their peak were 78 ± 5 ms (control; $n = 11$) and 61 ± 3 ms (*Rlbp1*$^{+/-}$*Gnat1*$^{-/-}$; $n = 9$; $P < 0.05$). Still, in both strains, the dim flash responses completely recovered to a baseline within 400 ms following the test flash of 2.4 × 10^3 photons μm^{-2}. Similarly, M-cone saturated responses appeared to be slightly faster in the mutant line (Fig. 2 D, inset). The mechanism producing this subtle difference in response kinetics is unclear. It is likely that it originates in cone phototransduction, as the kinetics of cone transretinal responses closely follow those recorded from individual cells by a suction electrode (Sakurai et al., 2011). However, it is also possible that the transretinal ERG responses are affected by voltage changes originating in the photoreceptor inner segments and axons (reviewed by Robson and Frishman, 2014). Importantly, the deletion of CRALBP did not cause any cone desensitization in CRALBP-deficient animals (Fig. 2 C).

Thus, the reduced CRALBP expression did not affect the overall health and function of dark-adapted cones and only accelerated moderately the inactivation of phototransduction in mouse M-cone photoreceptors in young adult mice. Overall, this allowed us to investigate the effect of decreased CRALBP level on dark adaptation of these cones as well as on their function in bright light.

Suppressed M-cone dark adaptation in mice with reduced expression of CRALBP

Cones constitute only a small fraction of the photoreceptors in most mammalian retinas, which makes it impossible to study their visual pigment regeneration and chromophore recycling by biochemical means. However, as the sensitivity of cones is

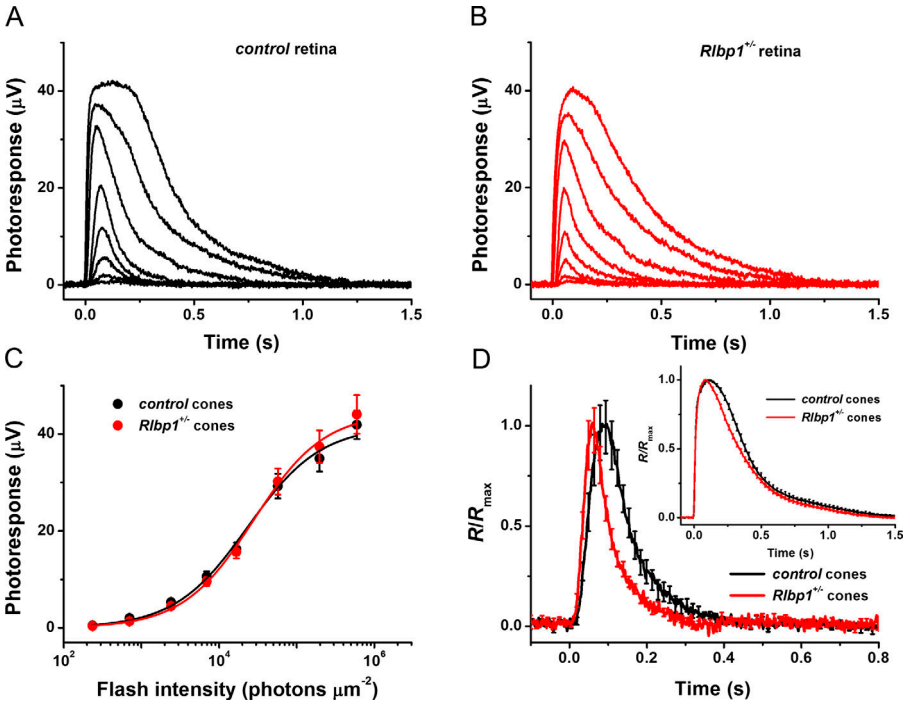

Figure 2. **Sensitivity ($I_{1/2}$) and kinetics of M-cone photoresponses in *Rlbp1*$^{+/-}$ mice. (A and B)** Representative families of M-cone transretinal ERG responses from 2-mo-old control *Gnat1*$^{-/-}$ (A) and *Rlbp1*$^{+/-}$*Gnat1*$^{-/-}$ (B) animals. Flash strengths were increased from 2.4 × 10^2 to 6.0 × 10^5 photons μm^{-2} by steps of ∼0.5 log units (505-nm light). **(C)** Averaged cone intensity–response functions (mean ± SEM) for isolated control *Gnat1*$^{-/-}$ (n = 10) and *Rlbp1*$^{+/-}$*Gnat1*$^{-/-}$ (n = 9) retinas. Points were fitted with Naka-Rushton hyperbolic functions (see Materials and methods). The fits yielded $I_{1/2}$ values of 2.4 × 10^4 and 2.8 × 10^4 photons μm^{-2} for control and mutant animals, respectively (P > 0.05). Error bars represent SEMs. **(D)** Population-averaged normalized dim flash cone responses (R/R_{max}) to test stimuli of 2.4 × 10^3 photons μm^{-2} for control *Gnat1*$^{-/-}$ (n = 11) and *Rlbp1*$^{+/-}$*Gnat1*$^{-/-}$ (n = 9) mice. The inset shows population-averaged normalized saturated cone responses to test stimuli of 6.0 × 10^5 photons μm^{-2} in the same retinas of the two mouse lines. Error bars represent SEMs.

strongly dependent on the level of visual pigment regeneration (Jones et al., 1989), it is possible to study the supply of chromophore to cones by the two visual cycles using measurements of cone sensitivity by electrophysiological recordings. In the case of mice, the electrical response generated by the cones (photopic ERG a-wave) is too small to be readily and reliably measured in vivo. Instead, we used the photopic ERG b-wave, a voltage signal recorded from the downstream bipolar cells, to monitor the sensitivity and, indirectly, the regeneration of pigment in mouse M-cones.

To address the possible role of CRALBP expression level in cone dark adaptation, we performed physiological experiments in live mice (Fig. 3). The recovery of M-cone S_f after acute (>90%) bleaching of cone visual pigment with 520-nm LED light (35-s exposure) was monitored in intact eyes with full-field ERG recordings. Under these noninvasive conditions, the photoreceptors remain in their native microenvironment and cone pigment regeneration is driven by the combined action of the visual cycles in RPE and Müller cells. First, we determined the b-wave sensitivity of dark-adapted cones (S_f^{DA}) and found that it was comparable in control (0.80 ± 0.02 m^2 cd^{-1} s^{-1}; n = 18) and *Rlbp1*$^{+/-}$ (0.90 ± 0.04 m^2 cd^{-1} s^{-1}; n = 20; P > 0.05) mice. We then used these respective dark-adapted values to normalize all subsequent measurements and derive relative recovery time courses. Following a nearly complete pigment bleach, cones initially were desensitized by ∼1.3 log units and then gradually recovered the bulk of their sensitivity in the dark. In this experiment, we found that the dark adaptation of M-cones after such acute pigment bleach was unaltered in *Rlbp1*$^{+/-}$ mice (Fig. 3 A) suggesting that the removal of approximately one-half of the CRALBP protein was insufficient to suppress the recovery of cone responsiveness in vivo.

The M-cone dark adaptation in the intact mouse eye is generally biphasic and the retina visual cycle contributes to its initial rapid phase (Kolesnikov et al., 2011), while a second (slower) component reflects visual pigment regeneration driven by the RPE visual cycle (Kolesnikov et al., 2015). However, more recent research has suggested that the interplay between the two phases of cone dark adaptation could be more complex in vivo (Kiser et al., 2018). To better dissect the role of CRALBP in maintaining the function of the retina visual cycle in live animals, MB-001, a potent selective RPE65 inhibitor of the retinylamine/emixustat family, was IP-injected into a cohort of mice, 22–26 h before performing similar ERG experiments. In our previous study, this drug effectively blocked the RPE visual cycle-driven component of cone sensitivity recovery (Kiser et al., 2018). Under these conditions, cone dark adaptation is driven exclusively by the intraretinal (Müller cell) visual cycle. The treatment did not change the S_f^{DA} in both control *Gnat1*$^{-/-}$ mice (0.75 ± 0.03 m^2 cd^{-1} s^{-1}; n = 18 in the treated cohort versus 0.61 ± 0.07 m^2 cd^{-1} s^{-1}; n = 8 in the untreated group; P > 0.05) and *Rlbp1*$^{+/-}$ mice (0.90 ± 0.04 m^2 cd^{-1} s^{-1}; n = 20 in the treated group versus 0.85 ± 0.03 m^2 cd^{-1} s^{-1}; n = 8 in the untreated cohort; P > 0.05). However, MB-001 unmasked the effect of the reduced CRALBP level on M-cone dark adaptation in *Rlbp1*$^{+/-}$ mice, which was suppressed under these conditions (Fig. 3 B). Thus, maintaining the proper level of CRALBP in Müller cells of the retina is important for the normal speed of visual pigment regeneration in mouse M-cones.

Prolonged bright light exposure further compromises the dark adaptation of M-cones in mice with reduced CRALBP expression

To gain further insight into the significance of CRALBP expression level for cone function in response to extended bright light in vivo, we performed the following ERG experiments. After recording the b-wave S_f of dark-adapted M-cones, we

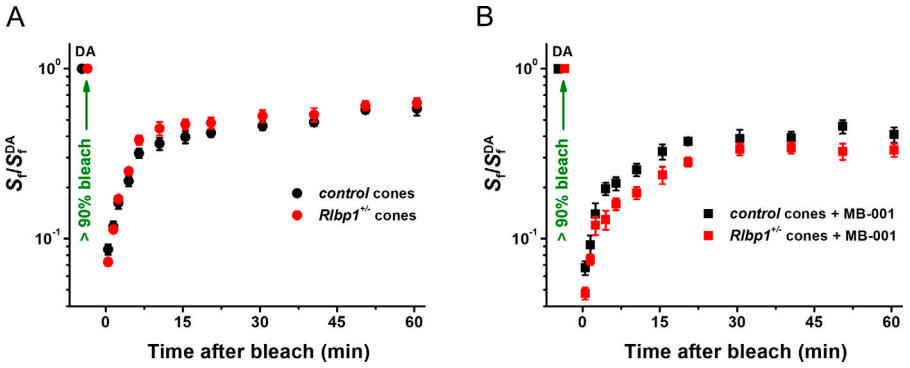

Figure 3. **M-cone dark adaptation measured from cone ERG b-wave in *Rlbp1*$^{+/-}$ mice in vivo. (A)** Recovery of cone ERG b-wave S_f (mean ± SEM) in control *Gnat1*$^{-/-}$ (n = 18) and *Rlbp1*$^{+/-}$*Gnat1*$^{-/-}$ (n = 20) mice after bleaching >90% of M-cone pigment at time 0 with 520-nm LED light. Two-way repeated-measures ANOVA did not reveal an overall significant effect of genotype ($F_{(1,36)}$ = 3.5; P = 0.07). DA refers to sensitivity of dark-adapted cones. **(B)** Recovery of cone ERG b-wave S_f (mean ± SEM) in control *Gnat1*$^{-/-}$ (n = 8) and *Rlbp1*$^{+/-}$*Gnat1*$^{-/-}$ (n = 8) animals injected with MB-001. Bleaching conditions were the same as in A. Two-way repeated-measures ANOVA showed an overall significant effect of genotype on recovery ($F_{(1,14)}$ = 6.0; P = 0.03). Error bars for some points in A and B are smaller than the symbol size.

applied a bright 530-nm Ganzfeld light (300 cd/m^2) for 30 min, which we estimated would bleach ∼0.8% of the M-cone pigment per second. This induced a rapid 2–log-unit cone desensitization due to background light adaptation (Fig. 4 A). In accordance with our earlier studies (Kolesnikov et al., 2015), we observed a small transient increase in cone b-wave S_f (presumably as a result of retina network adaptation) in both control and *Rlbp1*$^{+/-}$ animals. The short peak of S_f stability observed after 2–4 min of continuous illumination was then followed by its gradual decline. Although starting with somewhat lower sensitivity at the light onset, by the end of the background light exposure 30 min later, the cones in *Rlbp1*$^{+/-}$ mice were desensitized to an identical degree (216-fold relative to their dark-adapted state) to those in control animals (P > 0.05).

We then applied an additional bright 35-s 520-nm LED light to bleach the remaining M-cone pigment and afterward followed the recovery of photopic ERG b-wave sensitivity in the dark (Fig. 4 A, right; and Fig. 4 B). This allowed us to dissect a possible role of CRALBP level in dark adaptation of cone photoreceptors in a situation where any potential pools of cis-retinoids (in Müller cells and/or the RPE) available to dark-adapted cones should already be depleted. We observed that, similar to the case in human cones (Mahroo and Lamb, 2012), the overall rate of cone dark adaptation in control mice was decelerated substantially under these conditions, as compared with those treated with the equivalent 35-s bleaching under dark-adapted conditions (compare Fig. 4 B with Fig. 3 A). However, both the retina- and RPE-driven phases of cone dark adaptation were still unaffected in animals with reduced CRALBP expression in their eyes.

Finally, we repeated this experiment in mice pretreated with the blocker of the RPE visual cycle, MB-001 (Fig. 5). Although there was no overall statistically significant effect of this compound on M-cone sensitivity under extended bright light conditions over the 30-min period in *Rlbp1*$^{+/-}$ mice (Fig. 5 A), their subsequent dark adaptation was greatly compromised as compared with drug-treated controls (Fig. 5 B). Thus, our results demonstrate that the normal expression level of CRALBP in Müller cells is required for the proper function of the retina visual cycle and the efficient cone dark adaptation after intense illumination.

M-cones can maintain a moderate level of pigment regeneration in the absence of CRALBP

It was demonstrated recently that the complete elimination of CRALPB has a dramatic effect on the ability of the retina visual cycle to promote mouse cone dark adaptation, both in vivo and ex vivo (Xue et al., 2015). However, mouse M-cones were still

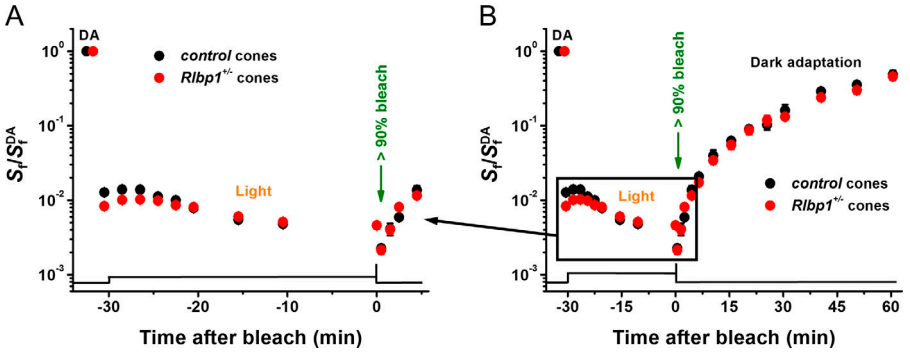

Figure 4. **Effect of extended light exposure on dark adaptation of M-cones measured from cone ERG b-wave in *Rlbp1*$^{+/-}$ mice in vivo. (A and B)** Change of photopic ERG b-wave S_f (mean ± SEM) following illumination with green 530-nm Ganzfeld background light (300 cd/m^2; 30 min; A) and its subsequent recovery in the dark after bleaching the bulk of the remaining cone pigment (B) in control *Gnat1*$^{-/-}$ (n = 6) and *Rlbp1*$^{+/-}$*Gnat1*$^{-/-}$ (n = 8) mice. S_f was normalized to its corresponding S_f^{DA} value in each case. Bleaching was induced by a 35-s illumination with bright 520-nm LED light at time 0. The time course of light exposure is shown on the bottom. Error bars for most points in A and B are smaller than the symbol size. Two-way repeated-measures ANOVA showed overall borderline significance of genotype on sensitivity during the extended light exposure ($F_{(1,12)}$ = 4.4; P = 0.058) but an insignificant effect during the subsequent recovery in the dark ($F_{(1,12)}$ = 0.6; P = 0.46). DA refers to sensitivity of dark-adapted cones.

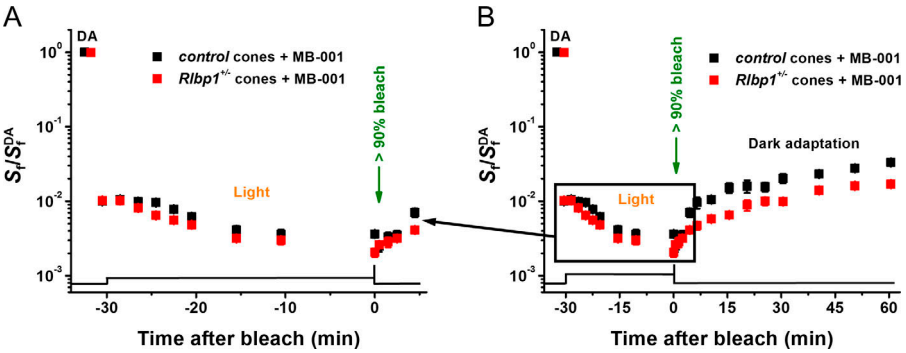

Figure 5. **Effect of extended light exposure on dark adaptation of M-cones measured from cone ERG b-wave in *Rlbp1*$^{+/-}$ mice in the presence of MB-001 in vivo. (A and B)** Change of photopic ERG b-wave S_f (mean ± SEM) following illumination with green 530-nm Ganzfeld background light (300 cd/m^2; 30 min; A) and its subsequent recovery in the dark after bleaching the bulk of the remaining cone pigment (B) in control *Gnat1*$^{-/-}$ (n = 10) and *Rlbp1*$^{+/-}$*Gnat1*$^{-/-}$ (n = 10) mice. S_f was normalized to its corresponding S_f^{DA} in each case. Bleaching was achieved by a 35-s illumination with bright 520-nm LED light at time 0. The time course of light exposure is shown on the bottom. Error bars for most points in A and B are smaller than the symbol size. Two-way repeated-measures ANOVA showed an overall insignificant effect of genotype on sensitivity during the extended light exposure ($F_{(1,18)}$ = 3.3; P = 0.09) but a highly significant effect during the subsequent recovery in the dark ($F_{(1,18)}$ = 20.1; P = 0.0003). DA refers to sensitivity of dark-adapted cones.

capable of restoring a considerable fraction (at least 0.5 log units) of their sensitivity in the absence of CRALBP in live animals. To address the possible existence of a CRALBP-independent mechanism of cone pigment regeneration in RPE cells, we used *Rlbp1*$^{-/-}$ mice that were either injected with MB-001 or untreated with the drug, to test their cone dark adaptation in vivo (Fig. 6).

Consistent with previous observations, we found a substantial (two- to threefold) decrease in photopic ERG b-wave S_f even in fully dark-adapted mice lacking CRALBP (Fig. 6 A, left). As expected, their cone dark adaptation after an acute, nearly complete pigment bleach was also greatly compromised (Fig. 6 A, red circles) compared with controls (Fig. 6 A, black circles). Similar to what we found in *Rlbp1*$^{+/-}$ animals described above, MB-001 did not reduce the maximal ERG b-wave amplitude (157 ± 11 µV; n = 8 in the treated group versus 166 ± 18 µV; n = 6 in the untreated mice; P > 0.05) or sensitivity (0.40 ± 0.05 m^2 cd^{-1} s^{-1}; n = 8 in the treated cohort versus 0.37 ± 0.03 m^2 cd^{-1} s^{-1}; n = 6 in the controls; P > 0.05) of dark-adapted M-cones in CRALBP-deficient mice. However, MB-001 suppressed further the cone post-bleach dark adaptation (Fig. 6 A, red squares), which could be visualized better after normalization of the data to the corresponding prebleach cone S_f (Fig. 6 B). The final level of response recovery by 60 min post-bleach in MB-001–treated *Rlbp1*$^{-/-}$ mice was approximately fourfold lower than in the control group, to which the compound was not administered. A small initial rapid component of cone S_f recovery (within 1 min after the bleach) still observed in treated mutant animals is likely due to the inactivation of the cone phototransduction cascade. Thus, the cone recovery from a bleach in CRALBP-deficient mice could be suppressed even further when the RPE visual cycle was blocked by MB-001. Together, these findings indicate that mouse M-cones can maintain a considerable level of their pigment regeneration through a yet to be identified shunt in the classical RPE visual cycle that bypasses CRALBP.

Dark adaptation of mouse rods is unaffected by reduced CRALBP expression

The results above clearly demonstrate the importance of maintaining the normal level of CRALBP protein in the eye for the function of mouse cones in bright light. Because the turnover of visual chromophore in the rod photoreceptors can affect pigment regeneration and dark adaptation in mammalian cones as well (Kolesnikov et al., 2015), we next investigated, with in vivo

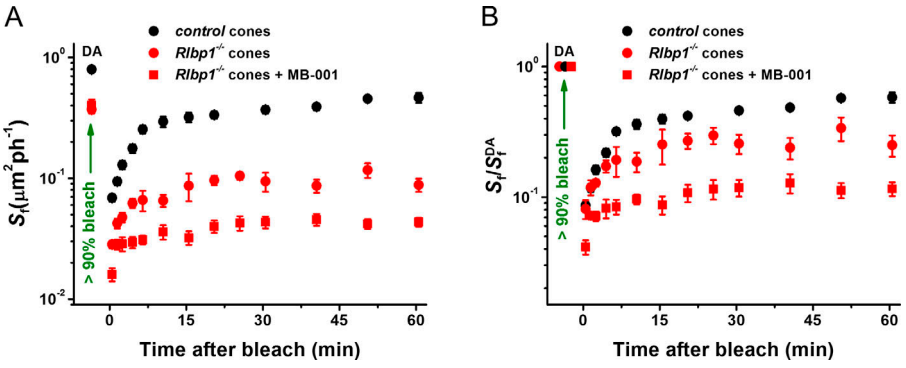

Figure 6. **Suppressed M-cone dark adaptation measured from cone ERG b-wave in *Rlbp1*$^{-/-}$ mice in the presence of MB-001 in vivo. (A)** Recovery of cone ERG b-wave S_f (mean ± SEM) in control *Gnat1*$^{-/-}$ (n = 18) and *Rlbp1*$^{-/-}$*Gnat1*$^{-/-}$ (n = 6) mice after bleaching >90% of M-cone pigment at time 0 with 520-nm LED light. Two-way repeated-measures ANOVA showed a highly significant effect of genotype on recovery ($F_{(1,22)}$ = 46.1; P < 0.0001). MB-001 (red squares) further suppresses cone dark adaptation in *Rlbp1*$^{-/-}$*Gnat1*$^{-/-}$ (n = 8) mice compared with untreated mutants ($F_{(1,12)}$ = 33.0; P < 0.0001). **(B)** The data in A were normalized to their own S_f^{DA} in each particular case. The effects of genotype and drug treatment remained highly significant after normalization ($F_{(1,22)}$ = 17.0; P = 0.0005; and $F_{(1,12)}$ = 14.4; P = 0.0025, respectively). Error bars for some points in A and B are smaller than the symbol size. DA refers to sensitivity of dark-adapted cones.

ERG recordings, whether the amount of CRALBP in the RPE modulates rhodopsin regeneration and dark adaptation of mouse rods. For rod recordings, *Rlbp1*$^{+/-}$*Gnat1*$^{+/-}$ and control *Rlbp1*$^{+/+}$*Gnat1*$^{+/-}$ lines were generated from an earlier established *Rlbp1*$^{-/-}$*Gnat1*$^{-/-}$ line. Mice with a *Gnat1*$^{+/-}$ genetic background that have nearly normal rod sensitivity and phototransduction (Calvert et al., 2000) were chosen for these experiments to facilitate the breeding scheme. We also performed a set of control rod dark adaptation experiments with wild-type animals from the same strain as the *Rlbp1*$^{+/-}$*Gnat1*$^{+/-}$ and *Gnat1*$^{+/-}$ mice used in our study. In these experiments, we found that both the level of rod ERG a-wave amplitude suppression and desensitization following an identical full pigment bleach were comparable in *Gnat1*$^{+/-}$ and control wild-type (*Gnat1*$^{+/+}$) mice, justifying our approach.

We first recorded rod-driven ERG responses in the dark and found that their waveforms and maximal amplitudes were comparable in control *Rlbp1*$^{+/+}$*Gnat1*$^{+/-}$ mice (338 ± 9 µV; n = 10) and animals with the halved expression of CRALBP (310 ± 16 µV; n = 10; P > 0.05; Fig. 7 A, bottom traces). The dark-adapted photosensitivities were also similar in the two mouse lines (1.37 ± 0.03 m^2 cd^{-1} s^{-1} versus 1.41 ± 0.08 m^2 cd^{-1} s^{-1}; P > 0.05), as well as rod ON bipolar cell-driven ERG b-waves. These findings demonstrate the normal function of rods in mutant mice in dark-adapted conditions. The kinetics of rod dark adaptation were then measured by monitoring the recovery of the rod ERG A_{max} and scotopic S_f after acute exposure to bright light that largely bleached (>90%) the rod pigment. As expected, immediately after bleaching, rods in both control and *Rlbp1*$^{+/-}$ mutants generated barely detectable ERG a-wave responses that were desensitized by almost 3 log units (Fig. 7 A, second traces from the bottom), which then recovered gradually over the following 60-min period of dark adaptation (Fig. 7 A, top three traces). The recovery of the averaged A_{max} in control rods could be described by a single-exponential function with a time constant of 38.8 ± 4.7 min (n = 10), and its level by 75 min after the bleach was ∼78% of the prebleach value (Fig. 7 B). The rate of rod dark adaptation was virtually identical in *Rlbp1*$^{+/-}$ mice (36.7 ± 3.6 min; n = 10; P > 0.05), and so was the final level of their maximal response amplitude after the bleach (79%). Similarly, no suppression of dark adaptation was observed in the recovery of the rod-driven ERG a-wave sensitivity following the same bleach (Fig. 7 C). Thus, the loss of approximately one-half of CRALBP protein was insufficient to compromise the regeneration of rhodopsin by the RPE visual cycle and the functional recovery of mouse rods in vivo.

Discussion

Efficient pigment regeneration plays a critical role in the ability of cone photoreceptors to function throughout the day in bright and rapidly changing light conditions. Mounting evidence indicates that this is achieved via parallel supplies with chromophore from the canonical visual cycle involving the RPE and from the retina visual cycle involving the Müller glial cells (Fleisch et al., 2008; Wang and Kefalov, 2009; Kolesnikov et al., 2011; Xue et al., 2015; Sato et al., 2017; Kiser et al., 2019; Morshedian et al., 2019; Ward et al., 2020). However, even though the functional significance of the retina visual cycle has now been well documented in a wide range of species, the molecular components of this pathway still remain largely unknown and controversial (Kaylor et al., 2013; Xue et al., 2017; Kiser et al., 2019; Ward et al., 2020). Here, we examined the role of one of these putative components, CRALBP. This chromophore-binding protein is expressed in both RPE and Müller cells (Bunt-Milam and Saari, 1983; Saari et al., 2001). A key feature of CRALBP is its binding selectivity for 11-cis-retinoids (Saari, 2012). As a result, in the RPE, it binds to 11-cis-retinol produced by RPE65, thus enhancing the recycling of chromophore by the RPE visual cycle (Winston and Rando, 1998; Stecher et al., 1999; Saari and Crabb, 2005; see also Fig. 8). Consistent with such a role, patients lacking functional CRALBP experience delayed dark adaptation (Burstedt et al., 2001) and a wide range of visual disorders.

The possible role of CRALBP in modulating the chromophore supply to cones is not well understood. It has been proposed that, similar to its function in the RPE, CRALBP expressed in Müller cells promotes the isomerization of all-trans-retinol back into its 11-cis form (Kaylor et al., 2013), but this has not yet been demonstrated experimentally in the retina. Another, not mutually exclusive alternative is that CRALBP in Müller cells serves as a storage site for recycled 11-cis-retinol, ready to be released and rapidly supplied to cones. Consistent with this notion, we have previously estimated that up to five CRALBP-associated 11-cis retinoids per cone pigment could be stored in Müller cells (Kiser et al., 2018). Thus, here we sought to evaluate how the expression level of CRALBP in both RPE and Müller cells affects the function of cones in dark-adapted conditions as well as during and after exposure to bright light bleaching a significant fraction of the cone visual pigment. These experiments allowed us to determine whether the expression level of CRALBP rate limits the ability of the RPE or the Müller cells to supply chromophore to cones in a timely fashion and to drive the efficient cone pigment regeneration.

Our results demonstrate that reducing twofold the expression of CRALBP in both the RPE and the Müller cells of *Rlbp1*$^{+/-}$ mice does not affect the dark-adapted photosensitivity of M-cones or the kinetics of cone dark adaptation following an acute bleach (Fig. 3 A). Similarly, the ability of these cones to function in continuous bright light or their subsequent dark adaptation following an acute bleach are also not compromised in *Rlbp1*$^{+/-}$ mice (Fig. 4). These results indicate that halving the expression of CRALBP does not slow down substantially the overall supply of chromophore to cones. However, as cone pigment regeneration in vivo is driven by the parallel function of two visual cycles, it is difficult to interpret this result in the context of each of the two pathways. Thus, we also examined separately how cone function is affected by the expression level of CRALBP in each visual cycle. Selective inhibition of the RPE visual cycle by a potent blocker of RPE65 activity, MB-001, allowed us to directly examine the effect of CRALBP expression in Müller cells on the efficiency of the retina visual cycle. We found that under these conditions the dark adaptation of M-cones following an acute pigment bleach (Fig. 3 B) and, to an even greater degree, their dark adaptation following an exposure to

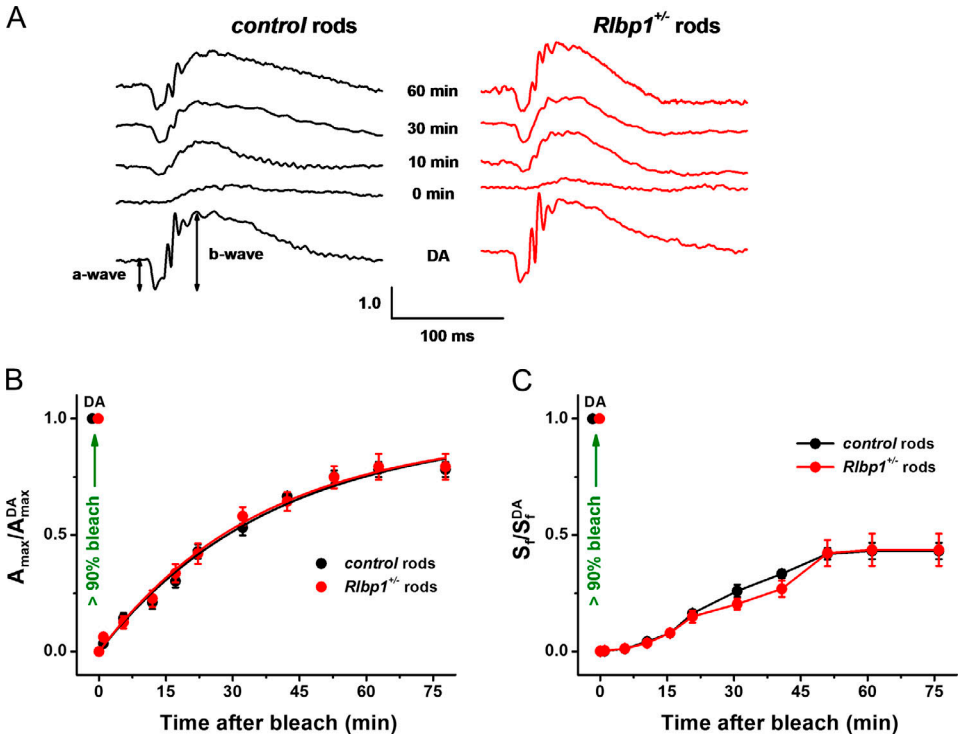

Figure 7. **Normal rod dark adaptation measured from rod ERG a-wave in *Rlbp1*$^{+/-}$ mice in vivo. (A)** Representative scotopic ERG responses in the dark (DA; bottom) and at four indicated time points after bleaching >90% of the rod pigment in control *Gnat1*$^{+/-}$ (left) and *Rlbp1*$^{+/-}$ (*Gnat1*$^{+/-}$; right) mice. For each time point, ERG A_{max} values were normalized to their corresponding prebleach dark-adapted value (A_{max}^{DA}). **(B)** Recovery of scotopic ERG A_{max} (mean ± SEM) after bleaching >90% of rhodopsin in control *Gnat1*$^{+/-}$ (n = 10) and *Rlbp1*$^{+/-}$ (*Gnat1*$^{+/-}$; n = 10) mice. Bleaching was achieved by a 35-s illumination with bright 520-nm LED light at time 0. Averaged data were fitted with single-exponential functions yielding time constants of 38.8 ± 4.5 min and 36.7 ± 3.6 min for control and *Rlbp1*$^{+/-}$ mice, respectively. Final levels of response recovery by 75 min post-bleach determined from exponential fits were 78% (control) and 79% (*Rlbp1*$^{+/-}$). An F test did not reveal a significant effect of genotype on the derived time constants or plateau values ($F_{(2,216)}$ = 0.19; P = 0.83). **(C)** Recovery of scotopic ERG a-wave S_f (mean ± SEM) after bleaching >90% of rod pigment in control *Gnat1*$^{+/-}$ (n = 10) and *Rlbp1*$^{+/-}$ (*Gnat1*$^{+/-}$; n = 10) mice. Two-way repeated-measures ANOVA showed an overall insignificant effect of genotype on recovery ($F_{(1,18)}$ = 0.18; P = 0.68). Animals and experimental conditions were the same as in B. Error bars for some points in B and C are smaller than the symbol size. DA refers to responses of dark-adapted rods.

continuous bright light (Fig. 5 B) were suppressed in *Rlbp1*$^{+/-}$ mice compared with controls. Together, these results clearly demonstrate that the expression level of CRALBP in Müller cells modulates the retina visual cycle (Fig. 8). The exact mechanism by which CRALBP in Müller cells affects the efficiency of cone pigment regeneration could involve transport of retinoids between cones and Müller cells, the recycling of retinoids in Müller cells, or their storage there. Notably, following dark adaptation, the function of cones in *Rlbp1*$^{+/-}$ mice recovered to normal even when the RPE visual cycle was blocked by MB-001. This is in stark contrast to the case of full CRALBP deficiency, where cone opsin is mislocalized and cone function is suppressed even after overnight dark adaptation (Xue et al., 2015).

Our experiments also allowed us to determine whether the RPE visual cycle is affected by the reduction in CRALBP expression. Since we still lack the tools to block selectively the retina visual cycle in vivo in a manner that would be nontoxic for Müller cells and other neurons in the retina, we were unable to evaluate directly the effect of CRALBP expression in the RPE on the efficiency of this visual cycle in providing chromophore to cones. However, the overall normal dark adaptation of cones in vivo when driven by both the RPE and retina visual cycles

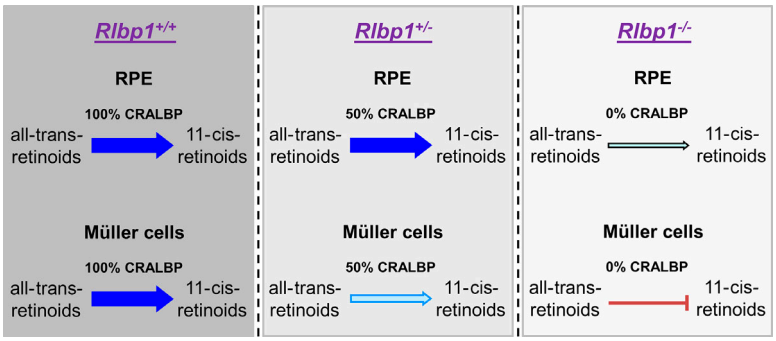

Figure 8. **Summary of our findings.** When expressed at normal levels, CRALBP promotes the recycling of 11-cis-retinoids in both the RPE and the Müller cells (left). Reducing the expression of CRALBP by twofold in *Rlbp1*$^{+/-}$ mice does not affect the efficiency of chromophore production by the RPE, but it suppresses its production by the Müller cells (middle). Finally, full deletion of CRALBP blocks the retina visual cycle, but recycling of chromophore still persists, albeit with reduced efficiency, via a CRALBP-independent shunt of the RPE visual cycle (right).

(Figs. 3 and 4) suggests that the RPE visual cycle efficiency is not compromised by reducing the expression of CRALBP there by twofold. A more direct examination of this question could be performed based on rod measurements, as rod pigment regeneration and dark adaptation are driven exclusively by the RPE visual cycle. Based on our finding that rod dark adaptation was comparable in control and *Rlbp1*$^{+/-}$ mice (Fig. 7), we conclude that the efficiency of the RPE visual cycle is not affected by halving the expression of CRALBP. Thus, the expression of CRALBP in the RPE is not rate limiting the recycling of chromophore by the RPE visual cycle and the pigment regeneration in either rods or M-cones (Fig. 8). We conclude that the CRALBP-driven delivery/release of chromophore to cones from the Müller cells modulates the retina visual cycle, whereas the corresponding step in the RPE does not regulate the canonical visual cycle. Interestingly, our observation of normal rod dark adaptation in *Rlbp1*$^{+/-}$ mice is in contrast to a previous study by Saari et al. (2001), who found a slight suppression in ERG a-wave recovery in *Rlbp1*$^{+/-}$ mice following a full bleach. The difference between these results is likely to originate in the RPE65 isoform of the mice used in the two studies. The mice in the original CRALBP-knockout mouse study were on the C57BL/6 background and most likely expressed the Met450 isoform of RPE65. In contrast, our mice were homozygous for the more active Leu450 isoform of RPE65, providing a more efficient chromophore regeneration by the RPE (Wenzel et al., 2001). A recent study demonstrated that short-wavelength fundus autofluorescence, which measures the presence of visual cycle–derived bisretinoids in the retina, was reduced in asymptomatic patients with heterozygous loss-of-function mutations in *RLBP1* (Lima de Carvalho et al., 2020). The lack of visual impairment in these individuals is consistent with our finding that classical visual cycle activity is normal in *Rlbp1*$^{+/-}$ mice. We speculate that the human fundus autofluorescence findings may reflect a subtle slowing of visual cycle activity that preferentially reduces off-pathway (i.e., bisretinoid-forming) reactions manifesting as an asymptomatic reduction in fundus autofluorescence.

Finally, our results also reveal a shunt in the classical RPE visual cycle that bypasses CRALBP and allows partial but surprisingly rapid M-cone dark adaptation (Fig. 6). This result is reminiscent of the finding that rods in CRALBP-deficient mice restore their visual chromophore and sensitivity following extended dark adaptation (Saari et al., 2001). Similarly, patients with compound heterozygous loss-of-function mutations in the *RLBP1* gene can also recover their rod-specific electroretinogram signals after overnight dark adaptation (Lima de Carvalho et al., 2020). Thus, the RPE visual cycle can function even in the absence of CRALBP and trickle-down chromophore not only to rods but also to cones (Fig. 8). The relatively fast dark adaptation of cones in CRALBP-deficient mice (Fig. 6) could likely be explained by the small amount of chromophore required for the regeneration of the visual pigment in these smaller and sparse (<3%; Carter-Dawson and LaVail, 1979) photoreceptors. In contrast, the much more abundant and larger rods require greater amounts of chromophore and thus take hours to dark adapt in the absence of CRALBP. Interestingly, this finding parallels the previously demonstrated ability of the retina visual cycle also to function, albeit suboptimally, even in the absence of CRALBP and to sustain cone survival in darkness in the absence of strong demand for chromophore (Xue et al., 2015).

Acknowledgments

David A. Eisner served as editor.

We thank Drs. John Saari (University of Washington, Seattle, WA) for providing *Rlbp1*$^{-/-}$ mice and the anti-CRALP antibody and Janis Lem (Tufts University School of Medicine, Boston, MA) for providing *Gnat1*$^{-/-}$ mice.

This work was supported by National Institutes of Health grants EY027283 (to K. Palczewski, P.D. Kiser, and V.J. Kefalov), EY009339 (to K. Palczewski), and EY002687 (to the Department of Ophthalmology and Visual Sciences at Washington University School of Medicine in St. Louis) and by a grant from the U.S. Department of Veterans Affairs (I01BX004939; to P.D. Kiser). The authors also acknowledge support from Research to Prevent Blindness unrestricted grants to the Department of Ophthalmology and Visual Sciences at Washington University of Medicine in St. Louis and the Department of Ophthalmology at the University of California, Irvine.

The authors declare no competing financial interests.

Author contributions: A.V. Kolesnikov, P.D. Kiser, K. Palczewski, and V.J. Kefalov contributed to the conception and design of this research. A.V. Kolesnikov and P.D. Kiser performed experiments and analyzed data. A.V. Kolesnikov, P.D. Kiser, K. Palczewski, and V.J. Kefalov wrote the manuscript. All authors approved the final version of the manuscript.

Submitted: 10 June 2020
Revised: 16 September 2020
Accepted: 27 October 2020

References

Bunt-Milam, A.H., and J.C. Saari. 1983. Immunocytochemical localization of two retinoid-binding proteins in vertebrate retina. *J. Cell Biol.* 97: 703–712. https://doi.org/10.1083/jcb.97.3.703

Burstedt, M.S., O. Sandgren, G. Holmgren, and K. Forsman-Semb. 1999. Bothnia dystrophy caused by mutations in the cellular retinaldehyde-binding protein gene (RLBP1) on chromosome 15q26. *Invest. Ophthalmol. Vis. Sci.* 40:995–1000.

Burstedt, M.S., K. Forsman-Semb, I. Golovleva, T. Janunger, L. Wachtmeister, and O. Sandgren. 2001. Ocular phenotype of bothnia dystrophy, an autosomal recessive retinitis pigmentosa associated with an R234W mutation in the RLBP1 gene. *Arch. Ophthalmol.* 119:260–267.

Burstedt, M.S., O. Sandgren, I. Golovleva, and L. Wachtmeister. 2003. Retinal function in Bothnia dystrophy. An electrophysiological study. *Vision Res.* 43:2559–2571. https://doi.org/10.1016/S0042-6989(03)00440-1

Calvert, P.D., N.V. Krasnoperova, A.L. Lyubarsky, T. Isayama, M. Nicoló, B. Kosaras, G. Wong, K.S. Gannon, R.F. Margolskee, R.L. Sidman, et al. 2000. Phototransduction in transgenic mice after targeted deletion of the rod transducin α-subunit. *Proc. Natl. Acad. Sci. USA.* 97:13913–13918. https://doi.org/10.1073/pnas.250478897

Carter-Dawson, L.D., and M.M. LaVail. 1979. Rods and cones in the mouse retina. I. Structural analysis using light and electron microscopy. *J. Comp. Neurol.* 188:245–262. https://doi.org/10.1002/cne.901880204

Eichers, E.R., J.S. Green, D.W. Stockton, C.S. Jackman, J. Whelan, J.A. McNamara, G.J. Johnson, J.R. Lupski, and N. Katsanis. 2002. Newfoundland rod-cone dystrophy, an early-onset retinal dystrophy, is caused by splice-junction mutations in RLBP1. *Am. J. Hum. Genet.* 70: 955–964. https://doi.org/10.1086/339688

Fleisch, V.C., H.B. Schonthaler, J. von Lintig, and S.C. Neuhauss. 2008. Subfunctionalization of a retinoid-binding protein provides evidence for two parallel visual cycles in the cone-dominant zebrafish retina. *J. Neurosci.* 28: 8208–8216. https://doi.org/10.1523/JNEUROSCI.2367-08.2008

Futterman, S., J.C. Saari, and S. Blair. 1977. Occurrence of a binding protein for 11-cis-retinal in retina. *J. Biol. Chem.* 252:3267–3271.

Grimm, C., A. Wenzel, D. Stanescu, M. Samardzija, S. Hotop, M. Groszer, M. Naash, M. Gassmann, and C. Remé. 2004. Constitutive overexpression of human erythropoietin protects the mouse retina against induced but not inherited retinal degeneration. *J. Neurosci.* 24:5651–5658. https://doi.org/10.1523/JNEUROSCI.1288-04.2004

He, X., J. Lobsiger, and A. Stocker. 2009. Bothnia dystrophy is caused by domino-like rearrangements in cellular retinaldehyde-binding protein mutant R234W. *Proc. Natl. Acad. Sci. USA.* 106:18545–18550. https://doi.org/10.1073/pnas.0907454106

Jones, G.J., R.K. Crouch, B. Wiggert, M.C. Cornwall, and G.J. Chader. 1989. Retinoid requirements for recovery of sensitivity after visual-pigment bleaching in isolated photoreceptors. *Proc. Natl. Acad. Sci. USA.* 86: 9606–9610. https://doi.org/10.1073/pnas.86.23.9606

Katsanis, N., N.F. Shroyer, R.A. Lewis, J.C. Cavender, A.A. Al-Rajhi, M. Jabak, and J.R. Lupski. 2001. Fundus albipunctatus and retinitis punctata albescens in a pedigree with an R150Q mutation in RLBP1. *Clin. Genet.* 59: 424–429. https://doi.org/10.1034/j.1399-0004.2001.590607.x

Kaylor, J.J., Q. Yuan, J. Cook, S. Sarfare, J. Makshanoff, A. Miu, A. Kim, P. Kim, S. Habib, C.N. Roybal, et al. 2013. Identification of DES1 as a vitamin A isomerase in Müller glial cells of the retina. *Nat. Chem. Biol.* 9:30–36. https://doi.org/10.1038/nchembio.1114

Kaylor, J.J., J.D. Cook, J. Makshanoff, N. Bischoff, J. Yong, and G.H. Travis. 2014. Identification of the 11-cis-specific retinyl-ester synthase in retinal Müller cells as multifunctional O-acyltransferase (MFAT). *Proc. Natl. Acad. Sci. USA.* 111:7302–7307. https://doi.org/10.1073/pnas.1319142111

Kaylor, J.J., T. Xu, N.T. Ingram, A. Tsan, H. Hakobyan, G.L. Fain, and G.H. Travis. 2017. Blue light regenerates functional visual pigments in mammals through a retinyl-phospholipid intermediate. *Nat. Commun.* 8:16. https://doi.org/10.1038/s41467-017-00018-4

Kiser, P.D., M. Golczak, and K. Palczewski. 2014. Chemistry of the retinoid (visual) cycle. *Chem. Rev.* 114:194–232. https://doi.org/10.1021/cr400107q

Kiser, P.D., J. Zhang, M. Badiee, Q. Li, W. Shi, X. Sui, M. Golczak, G.P. Tochtrop, and K. Palczewski. 2015. Catalytic mechanism of a retinoid isomerase essential for vertebrate vision. *Nat. Chem. Biol.* 11:409–415. https://doi.org/10.1038/nchembio.1799

Kiser, P.D., J. Zhang, A. Sharma, J.M. Angueyra, A.V. Kolesnikov, M. Badiee, G.P. Tochtrop, J. Kinoshita, N.S. Peachey, W. Li, et al. 2018. Retinoid isomerase inhibitors impair but do not block mammalian cone photoreceptor function. *J. Gen. Physiol.* 150:571–590. https://doi.org/10.1085/jgp.201711815

Kiser, P.D., A.V. Kolesnikov, J.Z. Kiser, Z. Dong, B. Chaurasia, L. Wang, S.A. Summers, T. Hoang, S. Blackshaw, N.S. Peachey, et al. 2019. Conditional deletion of Des1 in the mouse retina does not impair the visual cycle in cones. *FASEB J.* 33:5782–5792. https://doi.org/10.1096/fj.201802493R

Kolesnikov, A.V., S.A. Shukolyukov, M.C. Cornwall, and V.I. Govardovskii. 2006. Recombination reaction of rhodopsin in situ studied by photoconversion of "indicator yellow". *Vision Res.* 46:1665–1675. https://doi.org/10.1016/j.visres.2005.07.032

Kolesnikov, A.V., P.H. Tang, R.O. Parker, R.K. Crouch, and V.J. Kefalov. 2011. The mammalian cone visual cycle promotes rapid M/L-cone pigment regeneration independently of the interphotoreceptor retinoid-binding protein. *J. Neurosci.* 31:7900–7909. https://doi.org/10.1523/JNEUROSCI.0438-11.2011

Kolesnikov, A.V., A. Maeda, P.H. Tang, Y. Imanishi, K. Palczewski, and V.J. Kefalov. 2015. Retinol dehydrogenase 8 and ATP-binding cassette transporter 4 modulate dark adaptation of M-cones in mammalian retina. *J. Physiol.* 593:4923–4941. https://doi.org/10.1113/JP271285

Lima de Carvalho, J.R. Jr., H.J. Kim, K. Ueda, J. Zhao, A.P. Owji, T. Yang, S.H. Tsang, and J.R. Sparrow. 2020. Effects of deficiency in the *RLBP1*-encoded visual cycle protein CRALBP on visual dysfunction in humans and mice. *J. Biol. Chem.* 295:6767–6780. https://doi.org/10.1074/jbc.RA120.012695

Liu, T., E. Jenwitheesuk, D.C. Teller, and R. Samudrala. 2005. Structural insights into the cellular retinaldehyde-binding protein (CRALBP). *Proteins.* 61:412–422. https://doi.org/10.1002/prot.20621

Mahroo, O.A., and T.D. Lamb. 2012. Slowed recovery of human photopic ERG a-wave amplitude following intense bleaches: a slowing of cone pigment regeneration? *Doc. Ophthalmol.* 125:137–147. https://doi.org/10.1007/s10633-012-9344-z

Mattapallil, M.J., E.F. Wawrousek, C.C. Chan, H. Zhao, J. Roychoudhury, T.A. Ferguson, and R.R. Caspi. 2012. The Rd8 mutation of the Crb1 gene is present in vendor lines of C57BL/6N mice and embryonic stem cells, and confounds ocular induced mutant phenotypes. *Invest. Ophthalmol. Vis. Sci.* 53:2921–2927. https://doi.org/10.1167/iovs.12-9662

Maw, M.A., B. Kennedy, A. Knight, R. Bridges, K.E. Roth, E.J. Mani, J.K. Mukkadan, D. Nancarrow, J.W. Crabb, and M.J. Denton. 1997. Mutation of the gene encoding cellular retinaldehyde-binding protein in autosomal recessive retinitis pigmentosa. *Nat. Genet.* 17:198–200. https://doi.org/10.1038/ng1097-198

Morimura, H., E.L. Berson, and T.P. Dryja. 1999. Recessive mutations in the RLBP1 gene encoding cellular retinaldehyde-binding protein in a form of retinitis punctata albescens. *Invest. Ophthalmol. Vis. Sci.* 40: 1000–1004.

Morshedian, A., J.J. Kaylor, S.Y. Ng, A. Tsan, R. Frederiksen, T. Xu, L. Yuan, A.P. Sampath, R.A. Radu, G.L. Fain, and G.H. Travis. 2019. Light-driven regeneration of cone visual pigments through a mechanism involving RGR opsin in Muller glial cells. *Neuron.* 102:1172–1183.e5. https://doi.org/10.1016/j.neuron.2019.04.004

Naz, S., S. Ali, S.A. Riazuddin, T. Farooq, N.H. Butt, A.U. Zafar, S.N. Khan, T. Husnain, I.M. Macdonald, P.A. Sieving, et al. 2011. Mutations in RLBP1 associated with fundus albipunctatus in consanguineous Pakistani families. *Br. J. Ophthalmol.* 95:1019–1024. https://doi.org/10.1136/bjo.2010.189076

Nikonov, S.S., R. Kholodenko, J. Lem, and E.N. Pugh Jr. 2006. Physiological features of the S- and M-cone photoreceptors of wild-type mice from single-cell recordings. *J. Gen. Physiol.* 127:359–374. https://doi.org/10.1085/jgp.200609490

Nymark, S., H. Heikkinen, C. Haldin, K. Donner, and A. Koskelainen. 2005. Light responses and light adaptation in rat retinal rods at different temperatures. *J. Physiol.* 567:923–938. https://doi.org/10.1113/jphysiol.2005.090662

Robson, J.G., and L.J. Frishman. 2014. The rod-driven a-wave of the dark-adapted mammalian electroretinogram. *Prog. Retin. Eye Res.* 39:1–22. https://doi.org/10.1016/j.preteyeres.2013.12.003

Saari, J.C. 2012. Vitamin A metabolism in rod and cone visual cycles. *Annu. Rev. Nutr.* 32:125–145. https://doi.org/10.1146/annurev-nutr-071811-150748

Saari, J.C., and L. Bredberg. 1982. Enzymatic reduction of 11-cis-retinal bound to cellular retinal-binding protein. *Biochim. Biophys. Acta.* 716:266–272. https://doi.org/10.1016/0304-4165(82)90277-X

Saari, J.C., and D.L. Bredberg. 1987. Photochemistry and stereoselectivity of cellular retinaldehyde-binding protein from bovine retina. *J. Biol. Chem.* 262:7618–7622.

Saari, J.C., and J.W. Crabb. 2005. Focus on molecules: cellular retinaldehyde-binding protein (CRALBP). *Exp. Eye Res.* 81:245–246. https://doi.org/10.1016/j.exer.2005.06.015

Saari, J.C., D.L. Bredberg, and N. Noy. 1994. Control of substrate flow at a branch in the visual cycle. *Biochemistry.* 33:3106–3112. https://doi.org/10.1021/bi00176a045

Saari, J.C., M. Nawrot, B.N. Kennedy, G.G. Garwin, J.B. Hurley, J. Huang, D.E. Possin, and J.W. Crabb. 2001. Visual cycle impairment in cellular retinaldehyde binding protein (CRALBP) knockout mice results in delayed dark adaptation. *Neuron.* 29:739–748. https://doi.org/10.1016/S0896-6273(01)00248-3

Sakurai, K., J. Chen, and V.J. Kefalov. 2011. Role of guanylyl cyclase modulation in mouse cone phototransduction. *J. Neurosci.* 31:7991–8000. https://doi.org/10.1523/JNEUROSCI.6650-10.2011

Sato, S., and V.J. Kefalov. 2016. cis Retinol oxidation regulates photoreceptor access to the retina visual cycle and cone pigment regeneration. *J. Physiol.* 594:6753–6765. https://doi.org/10.1113/JP272831

Sato, S., R. Frederiksen, M.C. Cornwall, and V.J. Kefalov. 2017. The retina visual cycle is driven by cis retinol oxidation in the outer segments of cones. *Vis. Neurosci.* 34:E004. https://doi.org/10.1017/S0952523817000013

Schneider, C.A., W.S. Rasband, and K.W. Eliceiri. 2012. NIH Image to ImageJ: 25 years of image analysis. *Nat. Methods.* 9:671–675. https://doi.org/10.1038/nmeth.2089

Sillman, A.J., H. Ito, and T. Tomita. 1969. Studies on the mass receptor potential of the isolated frog retina. I. General properties of the response. *Vision Res.* 9:1435–1442. https://doi.org/10.1016/0042-6989(69)90059-5

Stecher, H., M.H. Gelb, J.C. Saari, and K. Palczewski. 1999. Preferential release of 11-cis-retinol from retinal pigment epithelial cells in the

presence of cellular retinaldehyde-binding protein. *J. Biol. Chem.* 274: 8577–8585. https://doi.org/10.1074/jbc.274.13.8577

Tang, P.H., M. Kono, Y. Koutalos, Z. Ablonczy, and R.K. Crouch. 2013. New insights into retinoid metabolism and cycling within the retina. *Prog. Retin. Eye Res.* 32:48–63. https://doi.org/10.1016/j.preteyeres.2012.09.002

Thompson, D.A., and A. Gal. 2003. Vitamin A metabolism in the retinal pigment epithelium: genes, mutations, and diseases. *Prog. Retin. Eye Res.* 22:683–703. https://doi.org/10.1016/S1350-9462(03)00051-X

Wang, J.S., and V.J. Kefalov. 2009. An alternative pathway mediates the mouse and human cone visual cycle. *Curr. Biol.* 19:1665–1669. https://doi.org/10.1016/j.cub.2009.07.054

Wang, J.S., and V.J. Kefalov. 2011. The cone-specific visual cycle. *Prog. Retin. Eye Res.* 30:115–128. https://doi.org/10.1016/j.preteyeres.2010.11.001

Ward, R., J.J. Kaylor, D.F. Cobice, D.A. Pepe, E.M. McGarrigle, S.E. Brockerhoff, J.B. Hurley, G.H. Travis, and B.N. Kennedy. 2020. Non-photopic and photopic visual cycles differentially regulate immediate, early, and late phases of cone photoreceptor-mediated vision. *J. Biol. Chem.* 295: 6482–6497. https://doi.org/10.1074/jbc.RA119.011374

Wenzel, A., C.E. Reme, T.P. Williams, F. Hafezi, and C. Grimm. 2001. The Rpe65 Leu450Met variation increases retinal resistance against light-induced degeneration by slowing rhodopsin regeneration. *J. Neurosci.* 21:53–58. https://doi.org/10.1523/JNEUROSCI.21-01-00053.2001

Winston, A., and R.R. Rando. 1998. Regulation of isomerohydrolase activity in the visual cycle. *Biochemistry.* 37:2044–2050. https://doi.org/10.1021/bi971908d

Woodruff, M.L., J. Lem, and G.L. Fain. 2004. Early receptor current of wild-type and transducin knockout mice: photosensitivity and light-induced Ca^{2+} release. *J. Physiol.* 557:821–828. https://doi.org/10.1113/jphysiol.2004.064014

Xue, Y., S.Q. Shen, J. Jui, A.C. Rupp, L.C. Byrne, S. Hattar, J.G. Flannery, J.C. Corbo, and V.J. Kefalov. 2015. CRALBP supports the mammalian retinal visual cycle and cone vision. *J. Clin. Invest.* 125:727–738. https://doi.org/10.1172/JCI79651

Xue, Y., S. Sato, D. Razafsky, B. Sahu, S.Q. Shen, C. Potter, L.L. Sandell, J.C. Corbo, K. Palczewski, A. Maeda, et al. 2017. The role of retinol dehydrogenase 10 in the cone visual cycle. *Sci. Rep.* 7:2390. https://doi.org/10.1038/s41598-017-02549-8

Zhang, J., E.H. Choi, A. Tworak, D. Salom, H. Leinonen, C.L. Sander, T.V. Hoang, J.T. Handa, S. Blackshaw, G. Palczewska, et al. 2019. Photic generation of 11-*cis*-retinal in bovine retinal pigment epithelium. *J. Biol. Chem.* 294:19137–19154. https://doi.org/10.1074/jbc.RA119.011169